

# LARGE-SCALE MAPPING OF FLOOD USING SENTINEL-1 RADAR REMOTE SENSING

M. H. Haghghi<sup>1,\*</sup>

<sup>1</sup> Institute of Photogrammetry and GeoInformation, Leibniz Universität Hannover, Germany - mahmud@ipi.uni-hannover.de

ICWG III/IVa

**KEY WORDS:** Monsoon Flood, Sentinel-1, Large-scale Mapping, Risk Assessment, Google Earth Engine

## ABSTRACT:

Sentinel-1 Synthetic Aperture Radar (SAR), with its extensive coverage and regular data acquisition all over the globe, has become one of the most valuable assets for flood monitoring in recent years. However, the strong influence of incidence angle on backscatter measurement of Sentinel-1 data makes it challenging to mosaic Sentinel-1 tracks for systematic flood mapping over large areas. This study uses a cosine squared normalization of Sentinel-1 data based on Lambert's law for optics to homogenize SAR data from different tracks. Then, it combines normalized data from ascending and descending passes forms 12-day mosaics covering Bangladesh from January 2017 to December 2021. Afterward, it estimates flood evolution by segmentation of the country-wide mosaics of data and calculates a flood frequency map. The flood frequency map, along with the population information, is then used to estimate the flood risk to the Bangladesh population. The results show that normalization can reduce inconsistencies between different tracks of Sentinel-1 data. Furthermore, it shows the potential of Sentinel-1 data for systematic flood mapping at large scales. Such analysis can help implement flood management measures on a national scale to reduce the flood risk.

## 1. INTRODUCTION

Remote sensing, with repeated satellite observations, provides a unique opportunity to assess the impact of flood disasters and support vulnerable people (Brakenridge et al., 2003; Klemas, 2014). Optical remote sensing data, e.g., Landsat, Sentinel-2, and MODIS, often face difficulties in mapping water because of cloud cover during the flood. Nevertheless, post-flood optical images are valuable because they can provide a picture of the damages and environmental situation (Gianinetto et al., 2006).

In contrast to optical remote sensing, Synthetic Aperture Radar (SAR) missions use microwaves and can penetrate clouds. Therefore, they observe the earth's surface during the flood and can regularly delineate flood extents (Schumann and Moller, 2015). Since the launch of the ERS-1 satellite in 1991, followed by the launch of a variety of sensors with different characteristics, SAR sensors have been widely used for flood mapping (Oberstadler et al., 1997; Bonn and Dixon, 2005; Henry et al., 2006; Martinis et al., 2015).

Since the launch of the Sentinel-1 mission in 2014, it has revolutionized the availability of SAR data by collecting images regularly across the globe. It collects SAR images in the same orbit every six days in Europe and every 12 days in other parts of the world. Furthermore, overlapping between frames and acquiring data in both ascending and descending orbits allow Sentinel-1 a repeat frequency of 1-4 days in many parts of the world (Potin et al., 2019).

In the past few years, different methods were developed and successfully used SAR backscatter data for delineating various flood events (Twele et al., 2016; Liang and Liu, 2020). The backscatter measurement of a SAR image depends on surface characteristics, i.e., surface roughness and dielectric constant of the soil. Water typically has a relatively smoother surface than soil or vegetation, resulting in lower backscatter values.

Therefore, it can be distinguished from land in SAR images (Schumann and Moller, 2015).

The backscatter measurement of SAR sensors, e.g., Sentinel-1, also depends on radar properties (polarisation and frequency) and sensor geometry (incidence angle). The radar frequency for a specific SAR mission is constant. Polarisation can also be considered constant for Sentinel-1 as the sensor acquires VV and VH polarisations in non-polar areas. On the other hand, incidence angle changes from 29° at near range to 46° at far range of Sentinel-1 images and alters the backscatter measurement within a frame of SAR image (Bauer-Marschallinger et al., 2021).

Sentinel-1 has become one of the most valuable assets for flood monitoring in the past few years. However, using Sentinel-1 data for systematic flood monitoring at large scales can still face two challenges. First is the large amount of SAR data that needs to be transferred and analyzed. The challenge of extensive data can be addressed using cloud-based platforms, such as Google Earth Engine. The Google Earth Engine platform hosts a rich archive of remote sensing data, including Sentinel-1. It allows the user to access the data and analyze them on the servers without transferring a large amount of data to the local computer (Gorelick et al., 2017). The Google Earth Engine platform has been used for flood mapping using optical and SAR data in recent years (DeVries et al., 2020; Singha et al., 2020).

The second challenge of using Sentinel-1 data for systematic flood mapping at large scales is the variations of incidence angle from near range to far range that can significantly affect the backscatter measurement. Furthermore, covering areas larger than a track width of Sentinel-1 (250 km) requires a mosaic of different tracks. On the other hand, floods typically change rapidly, and combining data from ascending and descending passes is required to increase the chance of capturing its extent. The variations of incidence angle, however, cause inconsistencies between the tracks.

\* Corresponding author

This study examines whether a normalization based on incidence angle improves the consistency of Sentinel-1 backscatter data for flood mapping at large scales. To do this, Bangladesh is chosen as a study area for two main reasons. First, flood is a country-wide problem in Bangladesh, and at least three different tracks of Sentinel-1 are required to cover the country entirely. Therefore, it allows the method suggested in this study to be examined. Second, Bangladesh is subject to repeated floods every year. Therefore, systematic flood monitoring is essential for the country.

This paper uses Google Earth Engine platform to analyze Sentinel-1 data to outline the flood history in Bangladesh from 2017 to 2021. First, a normalization based on incidence angle is performed to create uniform 12-day mosaics of SAR images. Then, the mosaic images are segmented into water and land. After that, a flood frequency map is calculated using the water extents. Finally, in combination with population density, the flood frequency map is used to estimate the risk of flood to the population.

The following section of the paper introduce the study area. Then, the methodology section describes the data and methods used for normalization of the data and delineating floods. After that, the results are provided, and the effectiveness of normalization and subsequent flood maps are discussed. Finally, the flood frequency and risk to the population are evaluated.

## 2. STUDY AREA

Bangladesh is a relatively small country in Southeast Asia with a population exceeding 160 million in an area of approximately  $148,000 \text{ km}^2$ . While 40% of the country's population lives in urban areas, Bangladesh has only two cities with populations larger than 1 million. Dhaka, the capital of Bangladesh, has a metropolitan population of nearly 22 million. More than 40% of the labor force work in the agriculture sector. Approximately 80% of the country's land consists of the fertile alluvial plain of large rivers with an elevation of roughly 20 m in the north, declining to the sea level in the south (Bangladesh, World Factbook, 2022).

Figure 1 shows the land cover and population density of Bangladesh. Three large rivers, Ganges, Jamuna, and Meghna, originating from the Himalayas and merging before flowing into the Bay of Bengal, create an alluvial plain in Bangladesh subject to frequent flooding. Monsoon rainfall, typically between June and October, affects Millions of people in Bangladesh every year and causes millions of dollars of damage to properties, infrastructure, crops, and livestock. Nevertheless, the flood control efforts in the past decades remained largely unsuccessful (Lewis, 2011).

Monsoon flood repeats every year in Bangladesh. In 2019, for example, it affected 5.4 million people and 37% of the country's area, and killed 26 people (Bangladesh: Monsoon Floods, 2021b). In 2020, more than a third of Bangladesh's total area was reported flooded. Approximately 5 million people were affected by prolonged floods, and 41 lost their lives. In addition, the damage to crops and livestock was estimated to be more than USD 40 and 70 million, respectively (Bangladesh: Monsoon Floods, 2021a).

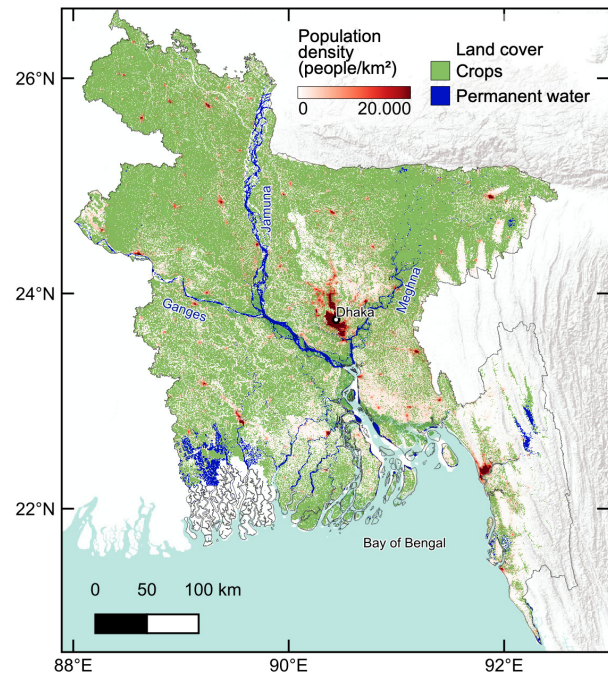


Figure 1. Land cover (crops and permanent water) and population density of Bangladesh overlaid on a shaded relief map. Three major rivers in Bangladesh are labeled. Population data from Tatem (2017), land cover data from Buchhorn et al. (2020), and shaded-relief map from Esri (2009).

## 3. METHODOLOGY

### 3.1 Dataset

Sentinel-1 Ground Range Detected (GRD) data, provided by European Space Agency, requires several pre-processing steps: applying orbit file, GRD border noise removal, thermal noise removal, radiometric calibration, and terrain correction. The resulting data is geocoded and calibrated to  $\sigma^0$  backscatter coefficient, which is the average radar cross-section per unit ground area (Filipponi, 2019). Because of its large dynamic range,  $\sigma^0$  is often expressed in the  $dB$  scale.

$$\sigma_{dB}^0 = 10 \log_{10}(\sigma^0) \quad (1)$$

This study uses Sentinel-1 GRD data available on Google Earth Engine platform (Gorelick et al., 2017). All pre-processing steps are already applied and the data is ready for flood analysis. The data is acquired in Interferometric Wide (IW) swath mode with a pixel size of  $10 \times 10 \text{ m}$  and a swath width of  $250 \text{ km}$ . Sentinel-1 data in Bangladesh are mainly acquired in dual polarisation: one co-polarisation (VV) and one cross-polarisation (VH). Google Earth Engine ingests Sentinel-1 to its archive with a time delay of two days.

Figure 2 illustrates the coverage of Sentinel-1 data in Bangladesh. The country is covered by three ascending and three descending tracks. Furthermore, there is an overlap between the tracks. Currently, Sentinel-1 collects data every 12 days in each track.

### 3.2 Normalization of backscatter coefficient

Before mosaicing images from different tracks and analyzing the flood, the SAR images are normalized to an arbitrary incidence angle. First, the backscatter coefficients are converted from the *dB*-scale to the original linear scale. Then, the values are normalized based on the pixel's incidence angles.

One of the common backscatter normalization techniques is based on Lambert's law for optics which assumes that the amount of backscattered energy from the surface follows a cosine law. Furthermore, the radiant variability as a function of the observed area depends on the cosine. Therefore, the backscatter coefficient of the image's pixel  $\sigma_{\theta}^0$  is related to the cosine squared of its incidence angle  $\theta$  (Mladenova et al., 2013; Topouzelis et al., 2016):

$$\sigma_{\theta}^0 = \sigma_0^0 \cos^2 \theta \quad (2)$$

where  $\sigma_0^0$  is the backscatter of the SAR pixel independent of the incidence angle. Consequently, the backscatter coefficient can be normalized to a reference incidence angle  $\theta_n$  as follows.

$$\sigma_{\theta_n}^0 = \sigma_{\theta}^0 \frac{\cos^2 \theta_n}{\cos^2 \theta} \quad (3)$$

In this study, backscatter coefficients are normalized to the reference incidence angle of  $35^{\circ}$ . After normalizing the backscatter coefficient, the values are converted back to the *dB* scale.

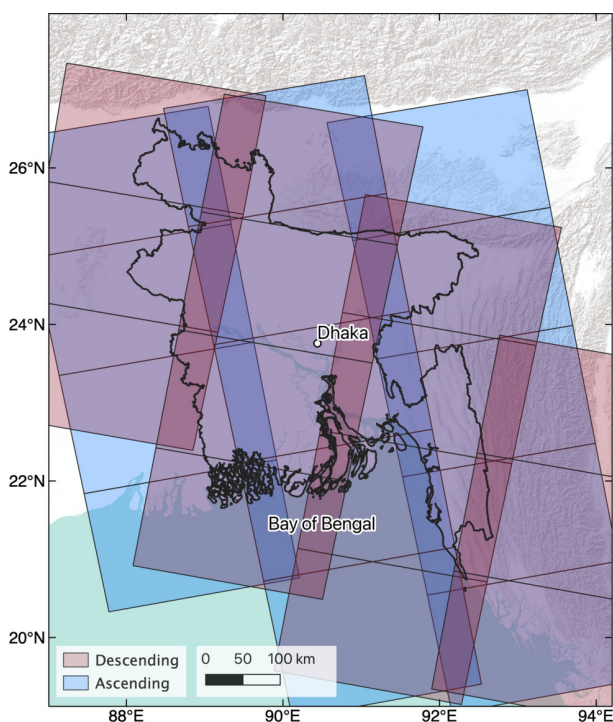


Figure 2. Coverage of Sentinel-1 ascending and descending tracks in Bangladesh overlaid on a shaded relief map. The black line delineates the boundary of Bangladesh. Shaded relief map from Esri (2009).

### 3.3 Mosaicing and filtering

Sentinel-1 data collected over 12-day periods in different ascending and descending tracks are merged to create extensive images covering the whole country. Overlapping between neighboring tracks or ascending and descending passes results in redundant data in various areas. The minimum value of images in overlapping areas is selected to obtain the lower backscatter coefficient over the 12 days and capture the maximum extent of the flood.

SAR images are inherently subject to speckle noise caused by interference of coherent waves from many distributed scatterers (Lee et al., 1994). In the past decades, different methods have been developed to reduce the speckle noise of SAR images. This study uses a simple median filter with a circle-shaped kernel of 100 meters, allowing a quick and efficient reduction of speckle noise.

### 3.4 Flood mapping

Typically, the backscatter coefficient of water is lower than soil and vegetation. Therefore, it is common to apply a threshold on the backscatter coefficient for segmentation of the SAR image to distinguish water from land (Matgen et al., 2011). In this study, a threshold of  $-16$  *dB* in VV polarisation is considered to delineate flood in 12-day mosaics. Then, a flood frequency map is generated from the 12-day flood maps.

## 4. RESULTS

### 4.1 Normalization results

This study demonstrates that the normalization of images based on incidence angle reduces the discrepancies between neighboring tracks. As an example, figure 3 shows a mosaic of three ascending tracks of Sentinel-1 acquired between 1 and 12 December 2021. There is an apparent trend in the backscatter coefficients correlated with the sensor's incidence angle. Generally, the backscatter coefficient values are higher at the near range and lower at the far range. As a result, there is a clear jump at the borders of the tracks, where the incidence angles suddenly change. After normalizing to an incidence angle of  $35^{\circ}$ , variations of backscatter coefficient with the incidence angle are less significant, and the jumps between the tracks are less apparent.

The correlation between backscatter coefficient and incidence angle is also confirmed in Figure 4-a. In this scatter plot, backscatter coefficient values averaged in 4-km cells are plotted against incidence angles. The scatter plot exhibits an obvious correlation. The best fit line has a negative slope with a  $-2.4$  *dB* difference in backscatter coefficient from the near range to the far range. Figure 4-b confirms that the normalization significantly reduced the correlation. The slope of the best fit line is less steep compared to the one from the original data, and the backscatter coefficient difference from the near range to the far range decreased to  $-0.6$  *dB*.

### 4.2 Flood mapping results

The evolution of flood across Bangladesh is estimated with a temporal resolution of 12 days. Figure 5 shows four examples of surface water extent in 2021 across Bangladesh identified based on segmentation of 12-day mosaics of Sentinel-1 normalized images. Comparison with Figure 1 suggests that in March,

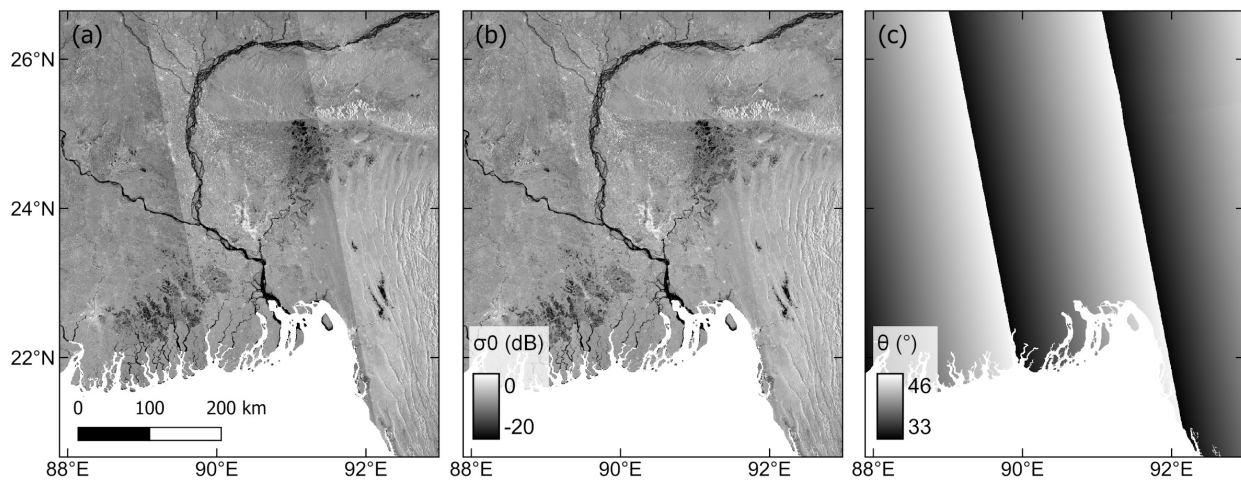


Figure 3. Image example of cosine squared normalization on three ascending tracks of Sentinel-1 VV polarisation in Bangladesh. The images are acquired between 1 and 12 December 2021. The ocean is masked out. (a) the original  $\sigma^0$  image. (b)  $\sigma^0$  image corrected to an incidence angle of  $35^\circ$ . (c) incidence angle.

mainly rivers and lakes are identified in the map and there is no significant flood. In June, an area in the northeast of the country is flooded. The flood area is extended in September. Finally, in December, a major part of flooded areas are drained, but there is still floodwater remaining in some areas.

Figure 6 indicates the flood frequency map between January 2017 and December 2021 across Bangladesh. As expected, permanent rivers (Ganges, Jamuna, and Meghna) and Kaptala lake have the highest flood frequency values. Therefore, permanent water from land cover maps (Buchhorn et al., 2020) is also shown on the map to distinguish them from actual floods. The flood frequency map suggests that flood repeatedly occurs in the country's northeast. In addition, along the three major

rivers, the river banks are also subject to frequent flooding.

To analyze the flooded areas across the country, permanent waters are masked out from the flood frequency map. The results indicate that 27% of the country's area (excluding permanent water) was inundated at least once from 2017 to 2021. The flood mainly affected rural areas rather than densely populated areas. Combining the prolonged flood map with population density information indicates the risk of flood to the population. Approximately 7% of the country's area has a flood frequency higher than 25%. 3% of the country's area is flooded more than half of the year, and 1% of the area is flooded more than three quarters of the year. Nearly 1 million people live in areas with flood frequency greater than 75%. More than 2 million of the population are affected by flood frequency greater than 50%, and

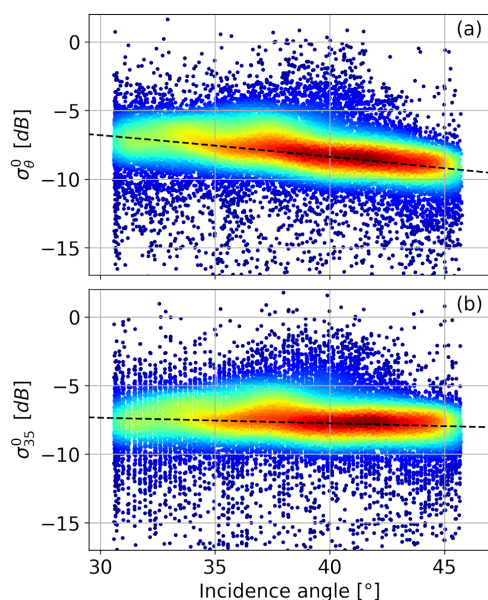


Figure 4. Dependency of backscatter coefficient on incidence angle in three tracks of Sentinel-1 data in ascending passes (shown in Figure 3). (a)  $\sigma^0$  before normalization and (b)  $\sigma^0$  after cosine squared normalization to an incidence angle of  $35^\circ$ . Dashed line represent the line of best fit.

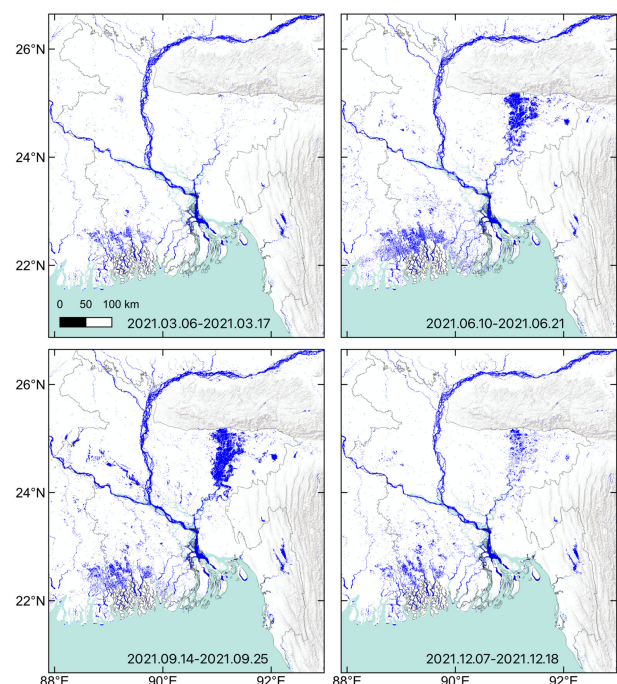


Figure 5. Water delineated in 12-day Sentinel-1 mosaics showing the evolution of flood in Bangladesh in 2021.

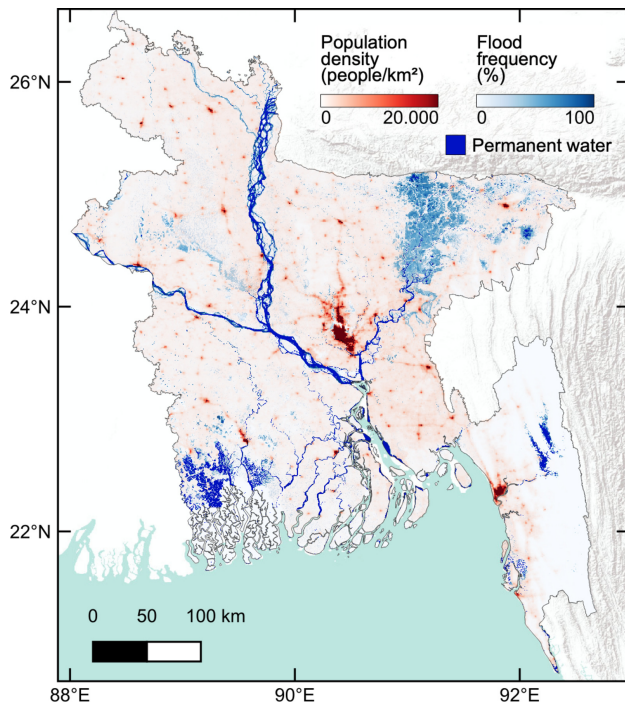


Figure 6. Flood frequency map of Bangladesh between January 2017 and December 2021. Population data from Tatem (2017), permanent water from Buchhorn et al. (2020).

more than 6 million live in areas with flood frequency higher than 25%.

## 5. CONCLUSION

This paper showed the capabilities of Sentinel-1 SAR images for systematic flood mapping at large scales. The Sentinel-1 GRD data were analyzed on the Google Earth Engine cloud computing platform. The data were normalized based on the cosine squared of incidence angle to produce a dataset with a homogeneous backscatter coefficient. Mosaics of SAR data in ascending and descending between January 2017 and December 2021 were generated and segmented to calculate 12-day flood maps. The 12-day flood maps were, then, used to calculate the flood frequency map. The result showed that approximately 30% of the country's area is inundated at least once during the 2017 to 2021 period.

The flood delineation is performed in this study using the segmentation of SAR images based on a uniform backscatter coefficient threshold as the most common flood delineation approach. However, other studies suggest more sophisticated segmentation methods, e.g., DeVries et al. (2020); Cian et al. (2018). Using such methods for segmentation of the normalized Sentinel-1 mosaics can improve the results and lead to more reliable flood mapping.

The study area investigated in this paper is relatively flat. Therefore, incidence angle is the main influencing factor on the backscatter coefficient. In areas with rough topography, topography variations with respect to the satellite's line of sight also affect the backscatter coefficient, particularly causing inconsistencies between ascending and descending tracks. Furthermore, radar shadow areas might be misinterpreted as floods in rough topography areas. Therefore, the local incidence angle should

be taken into account to correct the topography influence on the backscatter coefficient and construct homogeneous mosaics of Sentinel-1. Such methods for other applications are suggested, e.g., in Vollrath et al. (2020).

The flood frequency map produced in this study can be used as an estimate of flood probability in the future. Therefore, it is helpful for early warning and rescue planning. Further analysis can be performed based on the flood frequency map to assess flood risk to infrastructure, e.g., traffic network and food production, e.g., agriculture. The results can help implement flood management measures on a national scale to reduce the flood risk.

## ACKNOWLEDGEMENT

This paper contains modified Copernicus Sentinel data 2022. All maps are created by QGIS (QGIS Development Team, 2022).

## REFERENCES

- Bangladesh: Monsoon Floods, 2021a. Bangladesh: Monsoon Floods - Final Report (n° MDRBD022).
- Bangladesh: Monsoon Floods, 2021b. Bangladesh: Monsoon Floods - Final Report (n° MDRBD025).
- Bangladesh, World Factbook, 2022. Relief Central. Open Source Geospatial Foundation. <https://relief.unboundmedicine.com/relief/view/The-World-Factbook/563026/all/Bangladesh>.
- Bauer-Marschallinger, B., Cao, S., Navacchi, C., Freeman, V., Reuß, F., Geudtner, D., Rommen, B., Vega, F. C., Snoeij, P., Attema, E., Reimer, C., Wagner, W., 2021. The normalised Sentinel-1 Global Backscatter Model, mapping Earth's land surface with C-band microwaves. 8(1), 277. <https://doi.org/10.1038/s41597-021-01059-7>.
- Bonn, F., Dixon, R., 2005. Monitoring flood extent and forecasting excess runoff risk with RADARSAT-1 data. *Natural Hazards*, 35(3), 377-393.
- Brakenridge, G. R., Anderson, E., Nghiem, S. V., Caquard, S., Shabaneh, T. B., 2003. Flood warnings, flood disaster assessments, and flood hazard reduction: The roles of orbital remote sensing. *30th International Symposium on Remote Sensing of Environment, Honolulu, HI*.
- Buchhorn, M., Smets, B., Bertels, L., Roo, B. D., Lesiv, M., Tsendbazar, N.-E., Herold, M., Fritz, S., 2020. Copernicus Global Land Service: Land Cover 100m: collection 3: epoch 2019: Globe.
- Cian, F., Marconcini, M., Ceccato, P., 2018. Normalized Difference Flood Index for rapid flood mapping: Taking advantage of EO big data. *Remote Sensing of Environment*, 209, 712-730.
- DeVries, B., Huang, C., Armston, J., Huang, W., Jones, J. W., Lang, M. W., 2020. Rapid and robust monitoring of flood events using Sentinel-1 and Landsat data on the Google Earth Engine. *Remote Sensing of Environment*, 240, 111664.
- Esri, 2009. World Terrain Base [basemap]. Scale Not Given. "World Terrain Base". Jul 1, 2009. <https://www.arcgis.com/home/item.html?id=c61ad8ab017d49e1a82f580ee1298931>. (December 20, 2021).

- Filipponi, F., 2019. Sentinel-1 GRD preprocessing workflow. *3rd International Electronic Conference on Remote Sensing*, 18. <https://www.mdpi.com/2504-3900/18/1/11>.
- Gianinetto, M., Villa, P., Lechi, G., 2006. Postflood damage evaluation using Landsat TM and ETM+ data integrated with DEM. *IEEE Transactions on Geoscience and Remote Sensing*, 44(1), 236-243.
- Gorelick, N., Hancher, M., Dixon, M., Ilyushchenko, S., Thau, D., Moore, R., 2017. Google Earth Engine: Planetary-scale geospatial analysis for everyone. *Remote sensing of Environment*, 202, 18–27.
- Henry, J.-B., Chastanet, P., Fellah, K., Desnos, Y.-L., 2006. Envisat multi-polarized ASAR data for flood mapping. *International Journal of Remote Sensing*, 27(10), 1921-1929.
- Klemas, V., 2014. Remote Sensing of Floods and Flood-Prone Areas: An Overview. *Journal of Coastal Research*, 31(4), 1005-1013.
- Lee, J. S., Jurkevich, L., Dewaele, P., Wambacq, P., Oosterlinck, A., 1994. Speckle filtering of synthetic aperture radar images: A review. *Remote Sensing Reviews*, 8(4), 313-340.
- Lewis, D., 2011. *Bangladesh: politics, economy and civil society*. Cambridge University Press.
- Liang, J., Liu, D., 2020. A local thresholding approach to flood water delineation using Sentinel-1 SAR imagery. *ISPRS Journal of Photogrammetry and Remote Sensing*, 159, 53-62.
- Martinis, S., Kersten, J., Twele, A., 2015. A fully automated TerraSAR-X based flood service. *ISPRS Journal of Photogrammetry and Remote Sensing*, 104, 203-212.
- Matgen, P., Hostache, R., Schumann, G., Pfister, L., Hoffmann, L., Savenije, H., 2011. Towards an automated SAR-based flood monitoring system: Lessons learned from two case studies. *Physics and Chemistry of the Earth, Parts A/B/C*, 36(7), 241-252. Recent Advances in Mapping and Modelling Flood Processes in Lowland Areas.
- Mladenova, I. E., Jackson, T. J., Bindlish, R., Hensley, S., 2013. Incidence Angle Normalization of Radar Backscatter Data. *IEEE Transactions on Geoscience and Remote Sensing*, 51(3), 1791-1804.
- Oberstadler, R., Hönsch, H., Huth, D., 1997. Assessment of the mapping capabilities of ERS-1 SAR data for flood mapping: a case study in Germany. *Hydrological Processes*, 11(10), 1415-1425.
- Potin, P., Rosich, B., Miranda, N., Grimont, P., Shurmer, I., O'Connell, A., Krassenburg, M., Gratadour, J.-B., 2019. Copernicus sentinel-1 constellation mission operations status. *IGARSS 2019 - 2019 IEEE International Geoscience and Remote Sensing Symposium*, 5385–5388.
- QGIS Development Team, 2022. QGIS Geographic Information System. QGIS Association.
- Schumann, G. J.-P., Moller, D. K., 2015. Microwave remote sensing of flood inundation. *Physics and Chemistry of the Earth, Parts A/B/C*, 83-84, 84-95.
- Singha, M., Dong, J., Sarmah, S., You, N., Zhou, Y., Zhang, G., Doughty, R., Xiao, X., 2020. Identifying floods and flood-affected paddy rice fields in Bangladesh based on Sentinel-1 imagery and Google Earth Engine. *ISPRS Journal of Photogrammetry and Remote Sensing*, 166, 278-293.
- Tatem, A. J., 2017. WorldPop, open data for spatial demography. *Scientific Data*, 4.
- Topouzelis, K., Singha, S., Kitsiou, D., 2016. Incidence angle normalization of Wide Swath SAR data for oceanographic applications. *Open Geosciences*, 8(1), 450–464. <https://doi.org/10.1515/geo-2016-0029>.
- Twele, A., Cao, W., Plank, S., Martinis, S., 2016. Sentinel-1-based flood mapping: a fully automated processing chain. *International Journal of Remote Sensing*, 37(13), 2990-3004.
- Vollrath, A., Mullissa, A., Reiche, J., 2020. Angular-Based Radiometric Slope Correction for Sentinel-1 on Google Earth Engine. *Remote Sensing*, 12(11).